

Optical Transmission Losses in Polycrystalline Silicon Strip Waveguides: Effects of Waveguide Dimensions, Thermal Treatment, Hydrogen Passivation, and Wavelength

LING LIAO, DESMOND R. LIM, ANURADHA M. AGARWAL,
XIAOMAN DUAN, KEVIN K. LEE, and LIONEL C. KIMERLING

MIT, Materials Science and Engineering Department, Cambridge, MA 02139

Signal propagation delays dominate over gate delays in the ever-shrinking ultra large scale integrated (ULSI) circuits. Consequently, silicon-based monolithic optoelectronic circuits (SMOE) with their light speed signal propagation can provide unique advantages for future generations of microprocessors. For such SMOE circuits, we need optical interconnects compatible with silicon technology. Strip waveguides consisting of polycrystalline silicon (polySi) clad with SiO₂ offer excellent optical confinement and ease of fabrication that are ideal for such interconnect applications. One major challenge with using this material system, however, is its insertion loss. In this paper we provide techniques for minimizing optical transmission losses in polySi strip waveguides. Our previous work using polySi strip waveguides, showed an optical transmission loss of 15 dB/cm at $\lambda = 1.55 \mu\text{m}$, which is a communication wavelength of choice in optical fibers because it represents an absorption minimum. Similar measurements in crystalline silicon strip waveguides¹ yielded transmission losses of less than 1 dB/cm. Hitherto, in decreasing loss from 77 dB/cm to 15 dB/cm, we had minimized loss from surface scattering by improving the film surface morphology, and decreased bulk absorption with hydrogen passivation. In this paper we report a further reduction in the residual bulk loss from 15 dB/cm to 9 dB/cm. By experimenting with different waveguide core dimensions, we find that the contribution of bulk loss towards net transmission loss decreases with waveguide core thickness. Additionally, high temperature treatment provides strain relief in the polySi, decreasing transmission loss. Annealing in an oxygen ambient is not recommended because it always increases transmission loss. Hydrogen passivation improves transmission, attributable to passivation of light-absorbing dangling bond defect sites present at polySi grain boundaries. Together, these methods have resulted in the lowest measured loss value of 9 dB/cm at $\lambda = 1.55 \mu\text{m}$. Since integrated SiGe and Ge photodetectors are more efficient at shorter wavelengths like $\lambda = 1.32 \mu\text{m}$, transmission loss is also measured at $\lambda = 1.32 \mu\text{m}$. Losses at the two wavelengths (1.32 μm and 1.55 μm) are similar when defects and stress in the waveguides are minimized.

Key words: PolySi, strip waveguides, optical transmission loss

INTRODUCTION

As chip capabilities continue to increase, interconnect constraints are rapidly becoming the dominant limitation to chip speed. Important among the interconnect problems is accurate high frequency clock distribution, the transmission of the clock signal to all parts of the chip with minimal differential delays. As

clock speeds surpass the gigahertz level and clock skew is of the order of picoseconds, currently used electrical clock systems will require up to 200 watts of power and will use 2 billion lines/cm² of interconnect density.² To reach the Semiconductor Industry Association's (SIA) 0.1 μm gate-length goal for the year 2001, we need to use a combination of low dielectric constant isolation layers along with the copper metallization, to enable the transport of electrons at GHz speed.

(Received July 17, 2000; accepted August 15, 2000)

However, an excellent alternative to electrical interconnects are optical interconnects in silicon microphotonic circuits, because they offer high bandwidth, low power consumption, low noise, and reliable data transfer with minimal crosstalk, thereby allowing higher interconnection densities. Additionally, they introduce the signal transmission advantages of optics while maintaining the computational capabilities of electronics.

In our present work, we further investigate our previous proposal of polySi/SiO₂ waveguides for optical interconnects. The large refractive index contrast between the core and the cladding (3.5/1.5) enables excellent optical confinement, thus allowing sub-micron interconnect dimensions (0.5 μm or less) similar to the dimensions of conventional electrical interconnect lines.³ Additionally, polySi is used as the gate electrode in metal-oxide-semiconductor devices, the active layer in thin film transistors, and the high-value resistor in static memory circuits.^{4,5} A significant advantage of polySi interconnect material over single-crystalline silicon material, such as bonded and etched back silicon on insulator (BESOI), silicon implanted with oxygen (SIMOX), or silicon implanted with hydrogen and cleaved (ULTRABOND or SMARTCUT), is its ease of extension to multiple levels of interconnection. An added feature is that both the oxide cladding and silicon core thicknesses can be easily varied in polySi waveguides, whereas an upper bound exists on the oxide thickness in SIMOX structures and a lower bound exists in the core thickness in BESOI structures. ULTRABOND, which is really a better way of making smoother and more uniform BESOI, shares neither of the limitations of cladding or core thickness as seen in SIMOX or conventional BESOI. However, ULTRABOND technology is expensive at present. Therefore, although strip waveguide structures using crystalline technology yield transmission losses of less than 1 dB/cm,¹ polySi is still a desirable alternative to SIMOX, BESOI and ULTRABOND. Nevertheless, despite the ease of fabrication and flexibility offered by polySi optical interconnect technology, challenges in this material system remain to be addressed. Important among these limitations are photon scattering and photon absorption within the core and at the core/cladding interface, both of which lead to transmission losses in polySi/SiO₂ optical interconnects. In this paper, we discuss methods to improve the optical transmission properties of polySi/SiO₂ strip waveguides.

We evaluate the effects of waveguide thickness, thermal treatment and hydrogen passivation on relevant material and optical properties of polySi in an effort to lower the transmission losses. Transmission electron microscopy (TEM) and x-ray diffraction (XRD) are used to study the dependence of bulk loss on the size, structure, and quality of grains and grain boundaries. Secondary Ion Mass Spectrometry (SIMS) is used to study the level of hydrogenation in the samples. Two wavelengths of operation are investigated because they are the communication wavelengths of

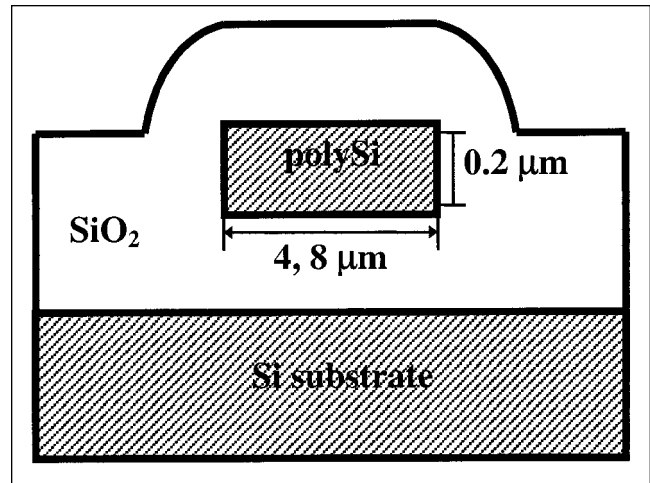


Fig. 1. The cross-sectional view of the experimental strip waveguide structure used to measure transmission losses in polySi. The polySi core is either 0.2 μm or 1 μm thick and 1, 2, 4, or 8 μm wide. The thickness of the oxide cladding under the polySi waveguide is about 1.8 μm and is obtained by thermal oxidation. The oxide above the polySi core is about 0.25 μm, deposited by low temperature oxidation. Transmission losses are measured in waveguides that are 8 μm in width.

choice in optical fibers: 1.55 μm is the absorption minimum and 1.32 μm is the dispersion minimum in optical fibers.

EXPERIMENT

The bottom cladding of the waveguides is formed by thermal oxidation of p-type, < 100 > silicon wafers to obtain 1.8 μm of SiO₂.³ This step is followed by the deposition of 0.2 μm or 1 μm of amorphous silicon at 560°C by using low pressure chemical vapor deposition (LPCVD). This process involves the pyrolytic decomposition of silane gas at a chamber pressure of 210 mtorr. The low 560°C deposition temperature is chosen as it yields smooth waveguides with an RMS roughness less than 4 nm after a recrystallization anneal and leads to 42 ± 2 dB/cm lower losses compared to polySi deposited at higher temperatures such as 625°C. Table I has a description of the polySi/SiO₂ interconnect sample labelling scheme. Each label indicates the thickness of the polySi core, the thermal anneal temperature and ambient, as well as the hydrogenation condition.

To crystallize these amorphous silicon films into polySi, the wafers are annealed for 16 h at 600°C in pure nitrogen, labeled as samples C[1 μm-600(N₂)] for the 1 μm polySi films or as samples E[0.2 μm-600(N₂)] for the 0.2 μm polySi films. To crystallize any residual amorphous silicon that may still remain in these films and to reduce any inter or intra-grain defects, an additional high temperature anneal is carried out for select wafers at 1100°C for 16 h in pure nitrogen leading to samples D[1 μm-600(N₂)+1100(N₂)] for the 1 μm polySi films and to samples F[0.2 μm-600(N₂)+1100(N₂)] for the 0.2 μm polySi films. To investigate the impact of anneal ambient, some wafers with a 1 μm thick polySi film are annealed in a mildly oxidizing ambient either at 600°C alone (samples A[1 μm-600(O₂)1], to com-

Table I. Labeling of Photolithographically Patterned Optical Interconnect Samples with PolySi Core and an SiO₂ Cladding*

Sample Label	Loss dB/cm	Thickness μm	Thermal Treatment Time/Temperature/Ambient	Hydrogen Passivation
A[1 μm -600(O ₂)]	37 \pm 6	1.0	16 h/600°C/(N ₂ +H ₂ O+O ₂)	None
A ₁ [A+ECR]	15 \pm 3			ECR
A ₂ [A+ECR+UST]	37 \pm 3			ECR + UST
A ₃ [A+PII]	28 \pm 2			PII
B[1 μm -600(O ₂)+1100(O ₂)]	High	1.0	[16 h/600°C/(N ₂ +H ₂ O+O ₂)+ 16 h/1100°C/(N ₂ +H ₂ O+O ₂)]	None
C[1 μm -600(N ₂)]	25 \pm 3	1.0	16 h/600°C/N ₂	None
D[1 μm -600(N ₂)+1100(N ₂)]	10 \pm 2	1.0	16 h/600°C/N ₂ + 16 h/1100°C/N ₂	None
EE[0.2 μm -600(O ₂)]	27 \pm 2	0.2	16 h/600°C/N ₂ +H ₂ O+O ₂	None
E[0.2 μm -600(N ₂)]	20 \pm 2	0.2	16 h/600°C/N ₂	None
E ₁ [E+R-ECR]	15 \pm 2			R-ECR
F[0.2 μm -600(N ₂)+1100(N ₂)]	11 \pm 2	0.2	[16 h/600°C/N ₂ + 16 h/1100°C/N ₂]	None
F ₁ [F+R-ECR]	9 \pm 2			R-ECR

* Samples are labeled according to their thickness, thermal treatment temperature and ambient, and hydrogen passivation conditions. Transmission loss measurements on these polySi optical interconnects were performed for each experimental condition using a standard cutback technique.⁸ The measured interconnects were 8 μm in width.

pare with samples C[1 μm -600(N₂)] or at, both, 600°C and 1100°C (samples B[1 μm -600(O₂)+1100(O₂)] to compare with samples D[1 μm -600(N₂)+1100(N₂)]. This mildly oxidizing ambient was calculated to have on the order of 10 torr of water vapor and 100 torr of oxygen in nitrogen, which yielded a 0.2 μm thick oxide after the 16 h 1100°C anneal.

The wafers are subsequently patterned into strips with widths of 1, 2, 4, and 8 μm and are reactive-ion-etched either in an SF₆ plasma or in HBr/Cl₂ plasma to obtain the rectangular polySi strip waveguide cores. Finally, a blanket layer of 0.25 μm SiO₂ is deposited to complete the oxide cladding and to protect the waveguide surface during the facet polishing required for transmission loss measurement. Figure 1 shows a schematic of the cross section of the resulting strip waveguides. Unpatterned wafers are cleaved into sections for materials characterization. Selected samples from both patterned and unpatterned batches are then hydrogenated to passivate dangling bonds which cause optical absorption and scattering of light. Four passivation techniques are investigated; they are electron cyclotron resonance (ECR) plasma hydrogenation, ultrasound treatment (UST) following ECR plasma hydrogenation, plasma ion implantation (PII) of hydrogen, and remote-source ECR (R-ECR) plasma hydrogenation. For ECR hydrogenation, samples A[1 μm -600(O₂)] are immersed in a high density hydrogen plasma at 350°C for 40 min with 600 W power and 0.16 mtorr pressure. These samples are then referred to as A₁ [A+ECR]. Studies have shown, however, that a considerable amount of the incorporated hydrogen atoms do not contribute to passivation because they

are weakly bound to one another instead of attaching to the silicon dangling bond.⁶ Low-temperature ultrasound treatment performed at 150°C for 30 min with a vibrational frequency of 400 kHz, is used for selected samples A₁ [A+ECR] to supply the additional activation energy needed for hydrogen-hydrogen bond separation⁶ followed by hydrogen-silicon bond formation. These samples are now labeled as samples A₂ [A+ECR+UST]. Another hydrogenation method investigated is plasma ion implantation (PII),⁷ a method that promises greater hydrogen incorporation than the ECR process by allowing high implantation doses of hydrogen. For the experiment, samples A[1 μm -600(O₂)] are implanted at 350°C with a dose rate of 2×10^{18} cm² sec and an energy of 2 keV and are then labeled as samples A₃ [A+PII]. The fourth hydrogenation condition is R-ECR plasma hydrogenation of samples. This technique minimizes possible surface damage from a plasma because the sample is placed away from direct ion exposure. The ions in the plasma are thus allowed to slow down before impacting the polySi film surface. For the R-ECR hydrogenation experiment, waveguides from samples E[0.2 μm -600(N₂)] and samples F[0.2 μm -600(N₂)+1100(N₂)] are exposed to a hydrogen plasma for 1 h at 100 W power, 0.33 torr pressure, and 350°C. These samples are then labeled as E₁ [E+R-ECR] and F₁ [F+R-ECR], respectively.

Optical transmission losses at $\lambda = 1.55$ μm and 1.32 μm are determined using a standard cutback technique.⁸ Light output from a diode source is coupled into a single-mode optical fiber. The fiber is then connected to a 90–10 power splitter: 90% of the power is butt-coupled into the waveguide under test, and 10% is directed to a multimeter where it is monitored

for voltage fluctuations. In order to factor out coupling loss and to determine the true transmission loss of the polySi structures, losses of several lengths of waveguides are measured.¹ The loss coefficient α is given by

$$\alpha = \left(\frac{\text{dB}}{\text{length}} \right) = \left(\frac{10}{L_1 - L_2} \right) \log \left(\frac{T_1}{T_2} \right) \quad (1)$$

where T_i is the ratio of the output power to the incident power for waveguides with length L_i . There is an estimated $\pm 5\%$ error on our measured values of α , arising from the error in length measurement.

The internal microstructure of polySi is examined using both TEM and XRD. Planview and cross-sectional TEM images are used to determine film crystallinity, grain structure, grain size, and intra-grain defects. For estimation of the grain size we use two techniques: a line technique⁹ and an area technique.¹⁰ For each sample, the techniques are repeated several times to obtain a mean grain size value. Using XRD, various films are analyzed for grain orientation and degree of crystallinity. Since the polySi films are at most $1 \mu\text{m}$ thick, a small x-ray incident angle is used to ensure that the beam does not penetrate to interact with the underlying oxide layer.

RESULTS AND DISCUSSION

Effect of Waveguide Thickness

First, to investigate the impact of waveguide dimension on optical transmission, the loss in sample C [$1 \mu\text{m}$ -600(N_2)] is compared to that in the thinner sample E [$0.2 \mu\text{m}$ -600(N_2)]. The second column in Table I lists the measured transmission losses in waveguides fabricated from each sample. Loss at $\lambda = 1.55 \mu\text{m}$ in the $1 \mu\text{m}$ thick sample C [$1 \mu\text{m}$ -600(N_2)] is $25 \pm 3 \text{ dB/cm}$ compared to the loss in the $0.2 \mu\text{m}$ thick sample E [$0.2 \mu\text{m}$ -600(N_2)] which is only $20 \pm 2 \text{ dB/cm}$, implying that the thinner waveguides show lower measured loss.

Additionally, we compare the measured loss with the simulated loss as a function of polySi waveguide thickness, as shown in Fig. 2. We see that our measurement agrees well with the numerical simulation. The simulation is based on confinement calculations and follows the trend that the loss decreases with decreasing thickness over a wide range of thicknesses. From these calculations, we attribute the reduced loss to the reduced overlap of the optical mode with the lossy core and an increased overlap with the less lossy oxide cladding. We attribute the overall loss reduction as polySi waveguide thickness decreases, to a tradeoff between three competing interactions. The modes in the thin ($0.2 \mu\text{m}$) waveguide extend out of the polySi core, compared to the modes in the thick ($1 \mu\text{m}$) waveguide: reducing the detrimental interaction with the lossy core; increasing the detrimental interaction with surface roughness; and finally, increasing the beneficial interaction with the less lossy underlying SiO_2 cladding.

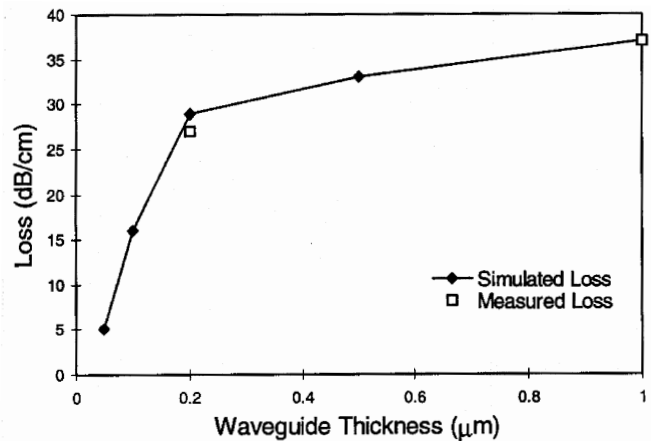


Fig. 2. Simulated and measured core (bulk) loss as a function of polySi waveguide thickness showing that core loss decreases with decreasing thickness. The measurement corresponds well with the simulation of loss as a function of waveguide thickness based on confinement calculations. (Courtesy A. Domnich and J.S. Foresi, private communication.)

Effect of Thermal Treatment (Temperature and Ambient)

Deposited amorphous silicon is recrystallized to polySi with a low temperature (600°C) heat treatment in a nitrogen ambient. When the heat treatment includes a high temperature (1100°C) anneal, local defects within the crystalline regions of the polySi waveguide are reduced, thereby improving transmission. An ambient of oxygen on the other hand converts some of the waveguiding regions, at the top surface as well as at the grain boundaries, to SiO_2 , and hence increases scattering losses.

0.2 μm Thick Waveguides

The deposited $0.2 \mu\text{m}$ thick amorphous-Si material is annealed at 600°C or at 600°C followed by another anneal at 1100°C , either in nitrogen with a small oxygen partial pressure or in pure nitrogen. This leads to four samples. However, the sample annealed at 1100°C in the oxygen partial pressure ambient was completely oxidized and was much too lossy to be of interest and so is not included in Table I.

X-ray diffraction (XRD) data from the other three samples, EE [$0.2 \mu\text{m}$ -600(O_2)], E [$0.2 \mu\text{m}$ -600(N_2)] and F [$0.2 \mu\text{m}$ -600(N_2)+1100(N_2)], are compared in Fig. 3a, b, and c, respectively. In Fig. 3a, which shows XRD peaks from sample EE [$0.2 \mu\text{m}$ -600(O_2)], the sample annealed at 600°C in an ambient with a small partial pressure of oxygen, some sharp peaks corresponding to the various crystal planes within the polySi are seen. Additionally, an amorphous SiO_2 peak is evident at $2\text{-Theta} = 18$. We attribute this broad peak to the SiO_2 within the grain boundaries in the bulk of the polySi core.

Samples E [$0.2 \mu\text{m}$ -600(N_2)] have been treated to a 16 h, 600°C recrystallization anneal in pure nitrogen. Note from Fig. 3b that the amorphous SiO_2 peak is not present in a nitrogen annealed sample as there is no oxygen in the ambient. Additionally, the XRD peaks

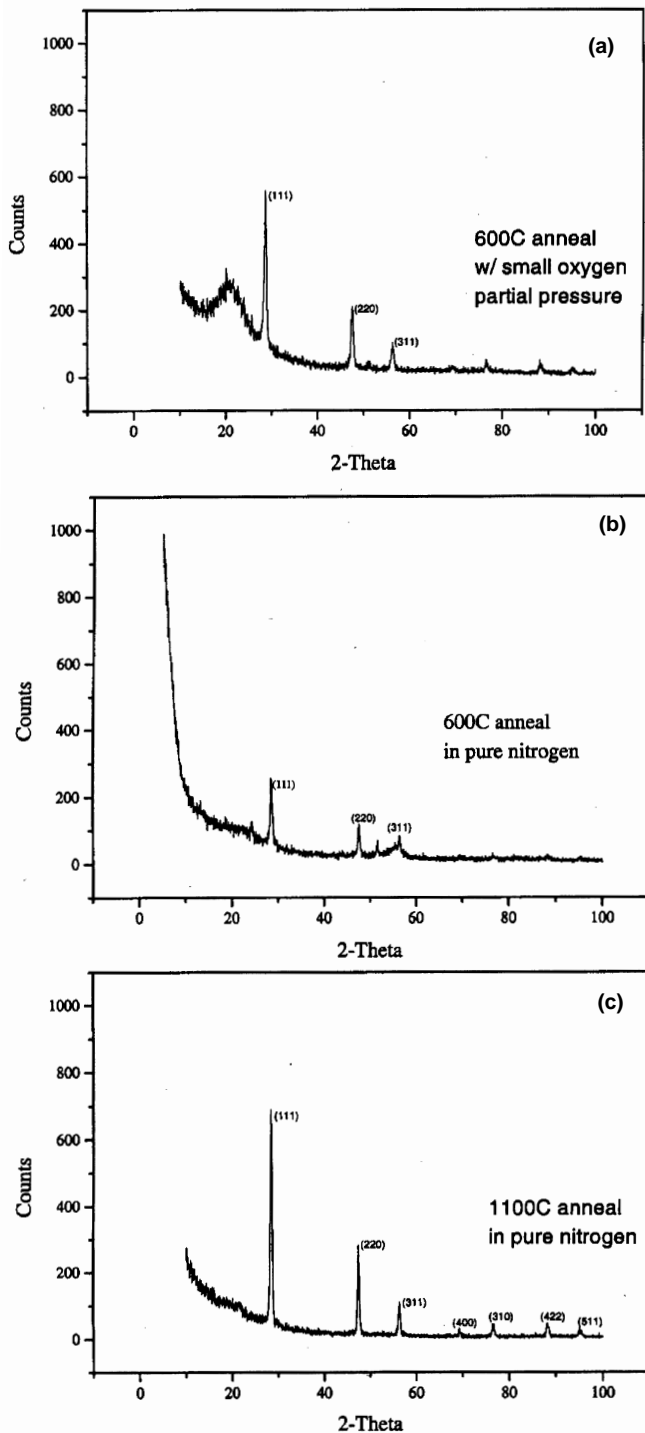


Fig. 3. X-ray diffraction curves of samples E[0.2 μm -600(N_2)], EE[0.2 μm -600(O_2)], and F[0.2 μm -600(N_2)+1100(N_2)]. In (a) corresponding to the XRD peaks from sample EE[0.2 μm -600(O_2)], the sample with a 600°C anneal in small oxygen partial pressure ambient, a broad amorphous peak is seen at $2\theta = 18^\circ$. In (b), showing the XRD peaks from sample E[0.2 μm -600(N_2)], the sample treated to a 600°C anneal in pure nitrogen, the lines corresponding to the silicon peaks are less sharp, compared to sample E[0.2 μm -600(N_2)]. This is attributed to strain present in these samples. Finally, in (c), showing XRD peaks from sample F[0.2 μm -600(N_2)+1100(N_2)], the sample with a 1100°C anneal in pure nitrogen, the amorphous peak has disappeared and the silicon peak lines are sharp again, possibly due to strain-relief provided by the high temperature treatment.

corresponding to diffraction from crystal planes are less sharp when compared to sample EE[0.2 μm -600(O_2)]. This broadening of the XRD peaks is attributed to strain. Strain induces a distribution of lattice constants in the nitrogen-annealed polySi material. Although transmission loss in sample E[0.2 μm -600(N_2)], at 20 dB/cm, is lower than in sample EE[0.2 μm -600(O_2)], at 27 dB/cm, we would like to identify the source of this loss and reduce it further. Since strain affects refractive index of polySi which in turn detrimentally impacts transmission of light, we attempt to improve transmission by providing strain-relief through a high temperature anneal at 1100°C. The results are seen in Fig. 3c, corresponding to XRD data from sample F[0.2 μm -600(N_2)+1100(N_2)]. Here we see sharper crystal plane peaks with a reduced background, attributed to strain relief, hence improved crystallinity. As expected, the transmission losses for waveguides annealed at the higher temperature decrease from 20 dB/cm to 11 dB/cm. Furthermore, cross-sectional transmission electron microscopy (XTEM) of sample F[0.2 μm -600(N_2)+1100(N_2)] confirms a reduction in both, the intragrain defect density and the grain boundary width, leading to an increase in the average grain size from 0.2 μm to 0.28 μm , when compared with sample E[0.2 μm -600(N_2)].

1 μm Thick Waveguides

From Table I, we can see that the effect of temperature and ambient are more pronounced in the 1 μm thick polySi waveguide samples, A[1 μm -600(O_2)], B[1 μm -600(O_2)+1100(O_2)], C[1 μm -600(N_2)], and D[1 μm -600(N_2)+1100(N_2)].

For example, in going from a 600°C anneal (sample A[1 μm -600(O_2)]: loss = 37 dB/cm) to a (600+1100)°C anneal (sample B[1 μm -600(O_2)+1100(O_2)]: loss = immeasurably high), both anneals in a partially oxidizing ambient, we notice a large difference in loss value. In the oxidizing ambient, we expect preferential oxidation of silicon, both, at the surface grain boundaries and at the grain boundaries within the waveguide core. The surface oxidation results in surface roughening and hence surface scattering. The bulk oxidation results in scattering of the optical modes at the boundary between the lower refractive index oxide and the higher refractive index silicon. Although this oxidation occurs in both samples, it is more significant in sample B[1 μm -600(O_2)+1100(O_2)], because oxygen diffusion, hence oxidation, is higher at 1100°C compared to 600°C.

A change in the ambient from partially oxidizing to inert, decreases transmission loss from 37 dB/cm (sample A[1 μm -600(O_2)]) to 25 dB/cm (sample C[1 μm -600(N_2)]). Therefore, although the diffusion of oxygen is small at 600°C, it is sufficient to make the loss in the partial oxidizing ambient 17 dB/cm higher.

Finally, a change in the anneal temperature from 600°C to (600 + 1100)°C brings the transmission loss down from 25 dB/cm (sample C[1 μm -600(N_2)] to 10 dB/cm (sample D[1 μm -600(N_2)+1100(N_2)]), again

attributable to strain-relief, hence improved transmission, at the higher temperature.

Effect of Hydrogen Passivation

Crystalline silicon has an energy gap of 1.1 eV; therefore, dangling bonds at grain boundaries in polySi can efficiently absorb both 0.8 eV and 0.9 eV radiation, corresponding respectively to 1.55 μm and 1.32 μm wavelength light. Absorption at dangling bond sites in the amorphous silicon, present either within the grain boundaries, or at defects within the grain, can lead to increased optical transmission losses. Several different hydrogenation processes are investigated as a means to reduce the effects of dangling bond defects and thus, transmission loss. The effectiveness of these techniques can be seen from Table I.

1 μm Thick Waveguides

Electron cyclotron resonance (ECR) passivation reduces the loss by 22 dB/cm in going from sample A₁[1 μm -600(O₂)] to sample A₁[A+ECR]. In this same sample, however, the process of (ultrasound treatment (UST) following the ECR, reverses the positive impact of ECR hydrogenation; increasing the loss back to 37 dB/cm (sample A₂[A+ECR+UST]). During the one hour UST process, the sample vibrates at 50 KHz supplying about 1 eV energy and the sample temperature reaches about 80°C. This high frequency vibration (50 KHz) could create micro-cracks in the polySi film, thereby reducing transmission.

The process of PII, with a high implantation dose (5×10^{16}) of hydrogen and high energy (45 KeV) plasma, offered an opportunity for greater hydrogen incorporation than the ECR method. However, the resulting samples A₃[A+PII] exhibit a transmission loss of 28 dB/cm, approximately 10 dB/cm higher than the best ECR result of 15 dB/cm of sample A₁[A+ECR]. Since the samples used for this experiment do not have a protective oxide layer, surface damage sustained during the impact of high velocity plasma constituents can explain the reduction in transmission. Hence further experiments with a protective oxide layer on the surface may be necessary to explore the advertised advantages of the PII technique.

0.2 μm PolySi Waveguides

Remote source ECR (R-ECR) plasma hydrogenation is a technique which minimizes ion impact damage to the surface of the waveguides because the sample is not located directly in the plasma. This technique is used to passivate samples E[0.2 μm -600(N₂)] and F[0.2 μm -600(N₂)+1100(N₂)] yielding sample E₁[E+R-ECR] and sample F₁[F+R-ECR], respectively. The resulting losses are 15 dB/cm in sample E₁[E+R-ECR] and 9 dB/cm in sample F₁[F+R-ECR].

Transmission loss decreases after hydrogenation by 22 dB/cm in sample A₁[A+ECR] and by 5 dB/cm in sample E₁[E+R-ECR], yielding the same final loss value of 15 dB/cm in both samples. This equivalence in loss value occurs despite the fact that A₁[A+ECR] is

Table II. Transmission Losses at $\lambda = 1.3 \mu\text{m}$ and 1.55 μm for Samples EE[0.2 μm -600(O₂)], E[0.2 μm -600(N₂)], E₁[E+R+ECR], and F[0.2 μm -600(N₂)+1100(N₂)]*

Sample Label	Loss (dB/cm)	
	1.32 μm	1.55 μm
EE[0.2 μm -600(O ₂)]	44 \pm 6	27 \pm 4
E[0.2 μm -600(N ₂)]	42 \pm 6	20 \pm 3
F[0.2 μm -600(N ₂)+1100(N ₂)]	16 \pm 3	11 \pm 2
E ₁ [E+R-ECR]	13 \pm 2	15 \pm 2

* Within the experimental error ($\pm 15\%$), losses are higher at $\lambda = 1.3 \mu\text{m}$ for samples EE[0.2 μm -600(O₂)], E[0.2 μm -600(N₂)], and F[0.2 μm -600(N₂)+1100(N₂)]. The higher loss is attributed to scattering from wavelength-dependent Rayleigh scattering sites, which appear to be somewhat neutralized after a high temperature treatment and entirely neutralized after hydrogen passivation. Transmission losses over a wider spectral range are currently underway to better understand this loss mechanism.

thicker, and is annealed in a low oxygen partial pressure ambient, both of which are detrimental to light transmission. One explanation for this equivalence, confirmed by SIMS hydrogen depth profiles, is that the R-ECR treatment results in lower H incorporation in sample E₁[E+R-ECR] than in the ECR-treated sample A₁[A+ECR]. An additional explanation is that the thinner 0.2 μm waveguides have fewer bulk defects (dangling bonds), and hence do not benefit as much from hydrogen passivation. Also, transmission in the 0.2 μm waveguides is very sensitive to surface and edge roughness. More experiments are underway to better understand the sources of this residual loss of 9 dB/cm in the 0.2 μm waveguides.

The R-ECR technique, coupled with the high temperature (1100°C) crystallization treatment of the 0.2 μm waveguide, gives the lowest reported polySi waveguide transmission loss of 9 dB/cm in sample F₁[F+R-ECR].

Transmission Losses at $\lambda = 1.32 \mu\text{m}$

Silicon germanium (SiGe) detectors which are compatible with polySi waveguide technology have been proposed and demonstrated by Giovane.¹¹ SiGe photodetectors are highly efficient absorbers at $\lambda = 1.32 \mu\text{m}$ and so transmission at this wavelength is investigated.

Table II compares the transmission losses at $\lambda = 1.32 \mu\text{m}$ and 1.55 μm . For samples EE[0.2 μm -600(O₂)] and E[0.2 μm -600(N₂)] transmission losses at $\lambda = 1.32 \mu\text{m}$ are 44 dB/cm and 42 dB/cm, respectively. They are each more than 20 dB/cm higher than the losses at $\lambda = 1.55 \mu\text{m}$ for the same two samples. This indicates that the ambient of the anneal is a less significant factor compared to the wavelength, in transmission losses.

To explain why we see greater transmission loss at $\lambda = 1.32 \mu\text{m}$ compared to $\lambda = 1.55 \mu\text{m}$, we must re-visit the sources of loss in polySi waveguides, namely, scattering and absorption losses. Absorption loss occurs due to electronic transitions between defect levels within the silicon bandgap. Scattering losses can

be categorized either as Rayleigh scattering losses or non-Rayleigh scattering losses. Rayleigh scattering loss is inversely related to the fourth power of the wavelength as shown in Eq. 2,

$$\alpha_{\text{scattering}} \propto \lambda^{-4} \quad (2)$$

Light of both wavelengths can cause absorptive loss transitions, indicating that scattering is the main source of the difference in loss. Furthermore, in polySi waveguides, localized variations of refractive index occur at defect sites. These variations act as random inhomogeneities causing Rayleigh scattering to be the predominant source of loss.

When sample E[0.2 μm -600(N₂)] is annealed at 1100°C for an additional 16 h, to yield sample F[0.2 μm -600(N₂)+1100(N₂)], the measured transmission loss at 1.55 μm decreases from 44 dB/cm to 11 dB/cm. At 1.32 μm the loss decrease is from 42 dB/cm to 16 dB/cm. The notable material changes resulting from the high temperature treatment are: improved degree of crystallinity, larger grain size, fewer grain boundaries and fewer dangling bonds. Hence, improved transmission at both $\lambda = 1.55 \mu\text{m}$ and 1.32 μm following the 1100°C anneal can be explained by a decrease in the number of absorption sites and Rayleigh scattering centers.

CONCLUSIONS

Transmission losses in polySi waveguides have been reduced by optimization of processing techniques. Thinner (0.2 μm) waveguides show lower losses than thicker (1.0 μm) waveguides, and this is attributed to lower bulk losses. A high temperature (1100°C) thermal treatment yielded lower losses than a lower temperature (600°C) anneal because of improved degree of crystallinity, larger grain size, fewer grain boundaries and fewer light-absorbing dangling bonds. Such thermal treatments in a pure nitrogen ambient show lower losses than in an oxygen partial pressure ambient, where oxidation of polySi occurs, especially at 1100°C. The oxide has a lower index of refraction compared to polySi and so when it replaces polySi within the waveguide, it leads to poorer confinement of light. Several kinds of hydrogenation techniques were used to passivate the dangling bonds

at the grain boundaries. Finally, transmission losses in polySi waveguides have been reduced to a best value of 9 dB/cm using a 1100°C anneal followed by R-ECR hydrogenation. Experiments are currently underway to isolate and explain this residual loss of 9 dB/cm.

ACKNOWLEDGEMENTS

The authors are grateful to Laura Giovane for initiating and facilitating the investigation of transmission losses at $\lambda = 1.3 \mu\text{m}$; to S. Ashok at Penn State University, for ECR plasma hydrogenation; to S. Ostapenko at University of South Florida for the ultrasound treatment following hydrogenation; to Chung Chan at Northeastern University for plasma ion implantation of hydrogen; and to Norbert Nickel at Hahn-Meitner Institute for remote ECR hydrogenation. This research was supported in part by Semiconductor Research Corporation (SRC) under Contract No. 94-SC-309 and the MRSEC program of the National Science Foundation under Award No. DMR-9400334.

REFERENCES

1. J.S. Foresi, M.R. Black, A.M. Agarwal, and L.C. Kimerling, *Appl. Phys. Lett.* 68, 2052 (1996).
2. L.C. Kimerling, D.M. Koker, B. Zheng, F.Y. Ren, and J. Michel, *Erbium-Doped Silicon for Integrated Optical Interconnects in Semiconductor Silicon*, ed. H.R. Huff, W. Bergholz, and K. Sumino (Pennington, NJ: The Electrochem. Soc., 1994), p. 486.
3. D.R. Lim, "Silicon Electro-Optic Modulator Based on Waveguide Coupling at $\lambda = 1.55 \mu\text{m}$ " (Bachelors thesis, MIT, 1994).
4. N. Yamauchi and R. Reif, *J. Appl. Phys.* 75, 3235 (1994).
5. D. Tsoukalas and D. Kouvatzos, *Appl. Phys. Lett.* 68, 1549 (1996).
6. S. Ostapenko, L. Jastrzebski, J. Lagowski, and R.K. Smeltzer, *Appl. Phys. Lett.* 68, 2873 (May 1996).
7. J.D. Bernstein, S. Qin, C. Chan, and T.-J. King, *IEEE Elec. Dev. Lett.* 16, 421 (October 1995).
8. L. Liao, "Low Loss Polysilicon Waveguides for Silicon Photonics" (Master's thesis, MIT, 1997).
9. T. Kamins, *Polycrystalline Silicon for Integrated Circuit Applications*, 2nd edition (Boston, MA: Kluwer Academic Publishers, 1991), p. 56.
10. D. Bisero, *Mater. Lett.* 18, 215 (1994).
11. L.M. Giovane, "Strain-Balanced Silicon-Germanium Materials for Near IR Photodetection in Silicon-Based Optical Interconnects" (Ph.D. thesis, MIT, 1998).